Extensive CO_2 emissions from shallow coastal waters during passage of Hurricane Irene (August 2011) over the Mid-Atlantic Coast of the U.S.A.

Citation	Crosswell, J. R., Wetz, M. S., Hales, B., & Paerl, H. W. (2014). Extensive CO_2 emissions from shallow coastal waters during passage of Hurricane Irene (August 2011) over the Mid-Atlantic Coast of the U.S.A. Limnology and Oceanography, 59 (5), 1651-1665. doi:10.4319/lo.2014.59.5.1651
DOI	10.4319/lo.2014.59.5.1651
Publisher	Association for the Sciences of Limnology and Oceanography, Inc.
Version	Version of Record
Terms of Use	http://cdss.library.oregonstate.edu/sa-termsofuse

Limnol. Oceanogr., 59(5), 2014, 1651–1665

doi:10.4319/lo.2014.59.5.1651

Extensive CO_2 emissions from shallow coastal waters during passage of Hurricane Irene (August 2011) over the Mid-Atlantic Coast of the U.S.A.

Joseph R. Crosswell,[1,2,*] Michael S. Wetz,[3] Burke Hales,[4] and Hans W. Paerl[1]

[1] Institute of Marine Sciences, University of North Carolina at Chapel Hill, Morehead City, North Carolina
[2] Department of Environmental Sciences and Engineering, University of North Carolina at Chapel Hill, Chapel Hill, North Carolina
[3] Department of Life Sciences, Texas A&M University at Corpus Christi, Corpus Christi, Texas
[4] College of Oceanic and Atmospheric Sciences, Oregon State University, Corvallis, Oregon

Abstract

Shallow coastal waters serve an important role as long-term carbon (C) sinks because they capture terrestrial C and retain internally produced C in wetlands and sediments. We show that tropical cyclones (TCs) can lead to rapid CO_2 efflux from estuaries, driven by physical and biogeochemical perturbation of these coastal C reservoirs, and that the magnitude of TC-driven CO_2 emissions may offset C that accumulates over much longer timescales. In August 2011, Hurricane Irene passed over North Carolina's Neuse River Estuary–Pamlico Sound (NRE-PS), which is part of the second largest estuarine system in the U.S., the Albemarle–Pamlico Sound. Irene rapidly changed the NRE-PS system from a small CO_2 sink to a large CO_2 source. Irene-induced CO_2 efflux from the NRE alone was at least four times the annual riverine C input and seven times the annual atmospheric CO_2 uptake. The magnitude and duration of ecosystem disturbance from TCs vary with storm intensity and frequency but likely are qualitatively similar across many terrestrial and coastal systems. Consequently, altered TC activity under future climate scenarios may shift the balance between C accumulation in, and release from, coastal C reservoirs.

Estuaries are highly active sites of carbon (C) transformation and exchange between land, ocean, and atmosphere. Estuaries receive ~ 50% of the terrestrial organic C (OC) that is input to inland waters, and the annual OC burial in coastal waters along the estuary–shelf continuum is approximately one third of the annual OC burial in the global ocean (Duarte et al. 2005; Regnier et al. 2013). However, the transport and processing of C in estuaries can be altered by climate-driven shifts in hydrology and physical perturbation by storms (Bauer et al. 2013; Wetz and Yoskowitz 2013). Tropical cyclones (TCs) are highly significant perturbations affecting estuarine biogeochemical processes (Paerl et al. 2006; Bauer et al. 2013), and recent climate models suggest TCs may become more intense but less frequent over the coming century (IPCC 2013). To project the effects of global climate change on estuarine biogeochemical dynamics and C storage capacity, it is imperative to first establish the magnitude and direction of C flux in response to TCs.

TC-driven perturbations potentially affect CO_2 fluxes in shallow coastal waters through two primary mechanisms. During the storm, extreme physical forcing increases air–water gas exchange and can release CO_2 from environments where atmospheric exchange is normally limited (McNeil and D'Asaro 2007; Huang and Imberger 2010; Ha and Park 2012). After the storm, hydrological forcing and input of organic matter (OM)– and nutrient-enriched waters alter the internal biogeochemical controls on estuarine C cycling (Hagy et al. 2006; Wetz and Yoskowitz 2013). Intense physical and biogeochemical perturbations by TCs have been observed in numerous coastal systems, but effects on air–water CO_2 fluxes have yet to be determined (Paerl et al. 2006; Sampere et al. 2008; DeLaune and White 2012). Here, we utilize observations of CO_2 partial pressure (P_{CO_2}) to quantify the effect of Hurricane Irene (2011) on air–water CO_2 flux in a large microtidal estuary, the Neuse River Estuary–Pamlico Sound (NRE-PS), North Carolina.

Methods

Study site—The NRE-PS is the largest component of the lagoonal Albemarle–Pamlico Sound (APS) system, which is made up of four subestuaries (NRE, PS, Pamlico River Estuary, Albemarle Sound), which are separated from the Atlantic Ocean by a chain of barrier islands having three narrow tidal inlets (Fig. 1). Limited exchange with coastal waters restricts tidal amplitudes to < 10 cm, and variations in water level are predominantly wind-driven as a result of the large fetch of the APS (Luettich et al. 2000). APS waters are weakly buffered, particularly during high river discharge, due to the low alkalinity and dissolved inorganic carbon (DIC) in feeder rivers (Crosswell et al. 2012).

Environmental setting—On 27–28 August 2011, Hurricane Irene (category 1 at landfall) passed directly over the NRE-PS, producing rainfall > 200 mm and sustained winds > 37 m s^{-1} (Fig. 1). The storm completely mixed the NRE-PS water column and continued on a path that affected the entire Mid- and north Atlantic Coast of the U.S. Wind-forcing drove high wave action and current velocities, and storm tides of up to 4 m flooded low-lying, C-rich wetlands (McCallum et al. 2012; Fig. 1). High rainfall in the NRE watershed led to a poststorm river discharge pulse that established a strong vertical salinity

* Corresponding author: jrc62@live.unc.edu

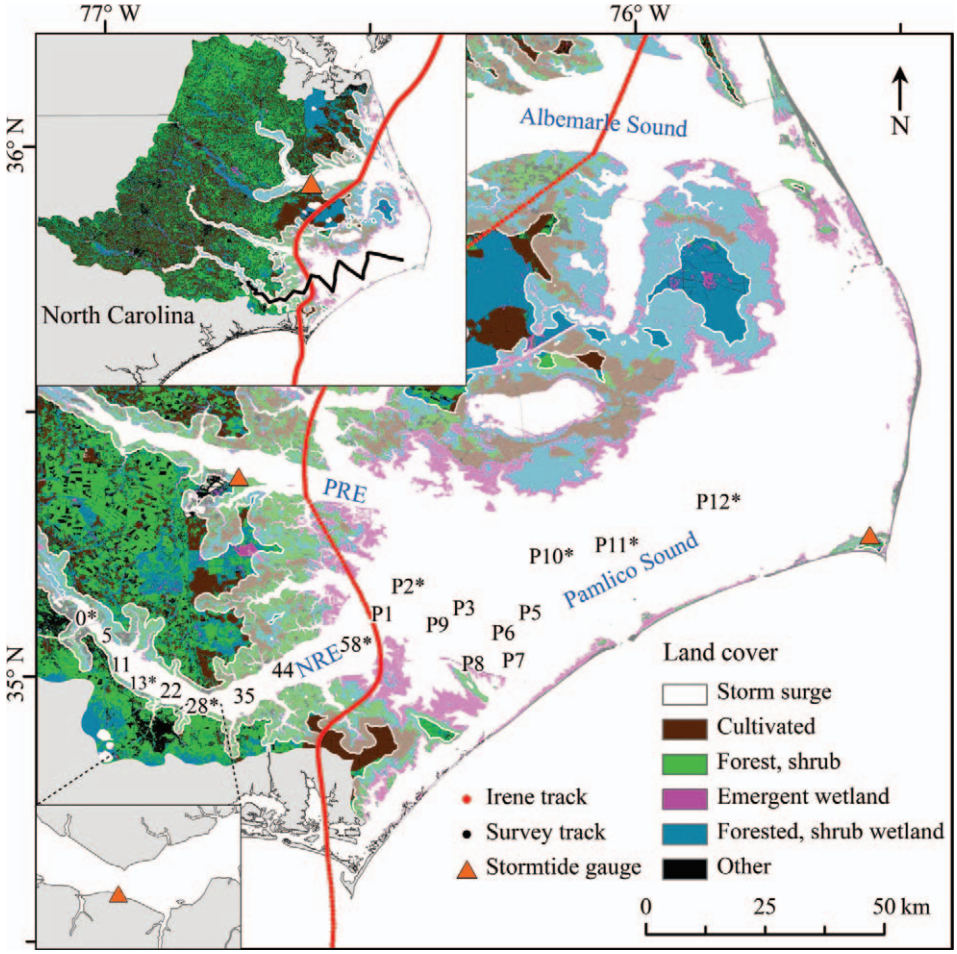

Fig. 1. P_{CO_2} survey track (top insert) and track of Hurricane Irene over APS waters: Neuse River Estuary (NRE), Pamlico River Estuary (PRE), Albemarle Sound, Pamlico Sound. NOAA Coastal Change Analysis Program land cover and ADCIRC-SWAN storm surge inundation data are projected over the APS watershed. NRE sampling locations are labeled by distance downstream from New Bern, North Carolina, and PS stations are labeled by order of collection. Sta. P10, P11, and P12 were sampled on the 14 September P_{CO_2} survey only. An asterisk denotes bottom-water P_{CO_2} sample locations on 14 September.

gradient, which persisted for 3 weeks following storm passage.

Surveys—The NRE-PS system has been intensively monitored for water-quality parameters for more than two decades as part of the NRE Modeling and Monitoring Project, ModMon (Paerl et al. 2001; Crosswell et al. 2012). In July 2009, NRE monitoring efforts were augmented to quantify CO_2 fluxes through high-resolution spatial surveys of surface-water CO_2 partial pressure (P_{CO_2}) and auxiliary parameters (surface temperature [ST], salinity, turbidity, dissolved oxygen [$O_{2(aq)}$], and chlorophyll *a* [Chl *a*]; Crosswell et al. 2012). In August 2010, the survey area was expanded to include the entire NRE (504 km^2), and separate surveys were conducted in the southern PS, over approximately one third of the total PS area (4418 km^2). Prior to Hurricane Irene, the NRE and PS surveys were combined and further extended to cover a surface area of ~4000 km^2 from Cape Hatteras on the Outer Banks to New Bern, North Carolina, at the mouth of the Neuse River (Fig. 1). Spatial surveys were conducted 3 d before and 1, 12, and 17 d after Hurricane Irene. Continuous along-track data were distance weighted to determine areal averages for P_{CO_2} and auxiliary parameters in the NRE and PS. P_{CO_2} surveys were conducted at approximately the same time of day, beginning at 14:00 h Coordinated Universal Time (UTC) in the PS and reaching the NRE by 17:00 h. Short across-axis P_{CO_2} surveys were also conducted near Sta. 28 during diurnal, wind-driven upwelling events (Reynolds-Fleming and Luettich 2004) on 25 August and 26 August, 1 and 2 d prior to Irene. ModMon surveys required 2 days to sample both the NRE and PS, with all surveys beginning at approximately 14:00 h. ModMon surveys were completed within 2 days of each P_{CO_2} survey.

Surface-water P_{CO_2} and auxiliary parameters were collected at a horizontal resolution of ~ 10 m using a flow-through system with a showerhead equilibrator and infrared gas analyzer onboard a small research vessel (Crosswell et al. 2012). During the 14 September 2011 P_{CO_2} survey, 17 d after the storm, bottom water was sampled by

Table 1. Method, wind speed range, and sampling period for $k(u_{10})$ parameterizations.

$k(u_{10})$ parameterization	Method	Wind speed* (m s^{-1})	Sampling period (d)
RC01, Raymond and Cole (2001)	Synthesis (floating dome)	0–7	
MH93, Marino and Howarth (1993)	Floating dome	0–10	9
P10, Prytherch et al. (2010)	Covariance	0–20	55†
E11, Edson et al. (2011)	Covariance	0–18	35
M01, McGillis et al. (2001)	Covariance	1–16	24
W09, Wanninkhof et al. (2009)	Synthesis	—‡	
W92, Wanninkhof (1992)	SF_6	1–7	14
J08, Jiang et al. (2008)	Synthesis	0–11	
H06, Ho et al. (2006)	^3He, SF_6	2–5	9
H11, Ho et al. (2011)	^3He, SF_6	8–16	21

* Average u_{10} over each measurement interval.
† 3938 20 min measurement intervals collected over 38 months.
‡ u_{10} range not reported.

connecting a pump to the flow-through intake and lowering a hose to 0.5 m above the sediment. These bottom-water samples were taken at the midpoint of each cross-axis transect in the PS and at Sta. 0, 13, 28, and 58 in the NRE (Fig. 1).

Gas-transfer velocity—Air–water CO_2 exchange is driven by the difference between the P_{CO_2} in the surface water and the atmosphere (ΔP_{CO_2}) scaled by the CO_2 gas solubility, and the rate of the exchange is set by the gas-transfer velocity of CO_2 (k). The transfer velocity is most commonly parameterized as a function of wind speed normalized to 10 m above the water surface (u_{10}). Large ranges of $k(u_{10})$ parameterizations have been identified through prior research (Wanninkhof et al. 2009), and it is prudent to apply a parameterization that appropriately represents the conditions observed during this study. We compare recent and widely used $k(u_{10})$ dependencies in Table 1 and Fig. 2 and justify our choice of parameterizations in the following paragraphs.

Three methods have been used to determine $k(u_{10})$ parameterizations: (1) small-scale measurement with a floating dome, (2) CO_2 covariance techniques, and (3) mass-balance estimates from the local release of gas tracers (Table 1). Floating dome studies typically derive steeper $k(u_{10})$ dependencies, which yield k values that we view as unrealistically high (e.g., > 10,000 cm h^{-1} at wind speeds of 25 m s^{-1} for the equation of Raymond and Cole, 2001) if extrapolated to the extreme wind speeds observed during Irene (Fig. 2). Relatively precise k measurements have been achieved using dual supersaturated gas tracers at low to moderate winds, but large uncertainties persist at high winds; widely used gas tracer parameterizations have been shown to underestimate air–water CO_2 fluxes in shallow coastal waters by as much as 90% due to enhanced gas exchange driven by wave breaking, bubbles, and bottom-generated turbulence (Woolf et al. 2007; Ho et al. 2014). Additionally, fluxes based on tracer budgets are integrated over a period of 12–24 h, which would underestimate peak gas exchange by nonlinear dependencies on high and highly variable winds, such as experienced during major storm events (Wanninkhof et al. 2009). The highest u_{10} range has been measured using CO_2 covariance methods (Table 1), which are able to resolve short-interval fluxes because 20–30 min measurement periods are binned by wind speed (Wanninkhof et al. 2009; Edson et al 2011). Accordingly, we estimated CO_2 fluxes using the $k(u_{10})$ parameterization of Prytherch et al. (2010), or "P10," because it is derived from what is currently the most extensive directly measured CO_2 flux data set, spanning the largest range of wind speeds (Table 1), and the CO_2 covariance method used by Prytherch et al. (2010) is the only method that represents high-wind fluxes on the short timescales of TC-driven forcing.

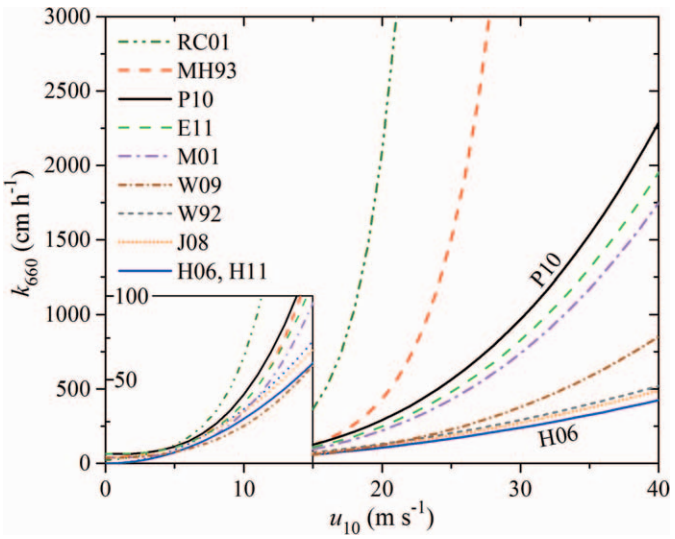

Fig. 2. Comparison of $k(u_{10})$ dependencies from Table 1 at $u_{10} < 15$ m s^{-1} (insert) and $u_{10} > 15$ m s^{-1}.

CO_2 fluxes are subject to large uncertainties, even in estuaries where gas exchange has been directly measured (Borges et al. 2004; Abril et al. 2009; Alin et al. 2011). For this reason, we have provided a lower bound for all CO_2 flux estimates using the $k(u_{10})$ parameterization of Ho et al. (2006) or "H06," which gives the lowest flux values of all widely used gas-transfer parameterizations (Fig. 2). CO_2 fluxes and C transport estimates are presented in the text as P10, with H06 listed subsequently in brackets: P10 (H06).

CO_2 fluxes—Spatially averaged air–water CO_2 fluxes were grouped into two time periods: the "during-storm"

period, representing the short-term effect of TC-force winds, and the "poststorm" period, reflecting longer-term effects of hydrological and biological forcing. The during-storm period was defined as the interval when the distance from the estuary center to Irene's wind center was < 500 km, the approximate radius of Hurricane Irene's sustained winds of > 10 m s^{-1}. This threshold was chosen based on prior observations that show the NRE-PS water column is typically well-mixed when sustained winds exceed ~ 10 m s^{-1} (Luettich et al. 2000; Whipple et al. 2006). The during-storm period lasted 43 h in the NRE and 42 h in the PS from 26 to 28 August 2011. The poststorm period ended on 14 September at the completion of the last P_{CO_2} survey. The total during- and poststorm study period was 20 d.

Air–water CO_2 fluxes were calculated according to Eqs. 1–3 using spatially averaged P_{CO_2}, salinity, and ST in the NRE and PS, hourly u_{10}, and the average atmospheric P_{CO_2} measured before and after each survey. The mole fraction of atmospheric CO_2 (xCO_2, μmol mol^{-1}) was converted to P_{CO_2} by multiplying by atmospheric pressure, a correction that was significant during the low ambient pressures associated with Irene.

$$\text{Flux} = K_0(k_{660})(\Delta P_{CO_2})(SC_{ST}/660)^{-0.5} \quad (1)$$

$$\text{P10} : k_{660} = 5.29 + 0.034u_{10}^3 \quad (2)$$

$$\text{H06} : k_{660} = 0.266u_{10}^2 \quad (3)$$

where K_0 is the CO_2 solubility coefficient (Weiss 1974), k_{660} is the gas-exchange coefficient (cm h^{-1}), ΔP_{CO_2} is the difference in CO_2 partial pressure between water and air (dPa), and Sc_{ST} is the Schmidt number for CO_2 at ambient ST and salinity (Wanninkhof 1992). All values were interpolated on hourly intervals between survey dates, except for during-storm P_{CO_2} and atmospheric pressure, for which interpolation methods are described below.

During-storm CO_2 fluxes were calculated using 2° u_{10} grids from the National Oceanic and Atmospheric Administration (NOAA) Atlantic Oceanographic and Meteorological Laboratory (AOML, http://www.aoml.noaa.gov/hrd/data_sub/wind.html). The u_{10} grid was spatially projected over the APS, and hourly winds were derived for each APS subsystem (NRE, PS, Pamlico River Estuary, Albemarle Sound) by averaging the 8 AOML grid points closest to the areal centroid of the respective region (determined using ArcGIS 10.0 geospatial analyst toolbox). Hourly data from the National Data Buoy Center (NDBC) Sta. CLKN7 at Cape Lookout, North Carolina, were used for all other time periods.

No measurements were made during Irene due to the clear risks of in-field observations, but recent modelling simulations indicate that high wind and current velocities mixed the vertically stratified water column and resuspended estuary sediments at the onset of the during-storm period (Brown et al. 2014; R. Corbett pers. comm.). We represent the concomitant input of high-P_{CO_2} bottom and pore water as a step increase in surface-water P_{CO_2}, based on in vitro simulations of P_{CO_2} during estuarine resuspension events (Abril et al. 2010). Surface P_{CO_2} was estimated using areally averaged data 1 day after the storm and corrected for hourly atmospheric pressure from NDBC Sta. CLKN7. This representation clearly simplifies the response of a shallow, weakly buffered estuary to extreme physical perturbation during a TC; we justify this stepwise approach as a conservative choice to estimate during-storm CO_2 flux and discuss relevant uncertainties in later sections.

C budget—We constructed a first-order water and C budget to determine if water-column CO_2 lost through air–water efflux could be actively replenished by vertical mixing and C input from river discharge, sediment resuspension, and nonriverine stormwater runoff. Hourly river discharge was obtained from two U.S. Geological Survey streamflow gauging stations (Neuse River 02091814, Trent River 02092500), both located approximately 20 km upstream from Sta. 0 (Fig. 1). Stormwater input was determined using rainfall data from the U.S. National Aeronautics and Space Administration Tropical Rainfall Measuring Mission (3B42 V7; http://trmm.gsfc.nasa.gov), assuming a 100% runoff coefficient. DIC, dissolved OC (DOC), and particulate OC (POC) concentrations in river and stormwater input were assumed to be equal to the DIC, DOC, and POC concentration of the freshwater sample at Sta. 0 on 30 August 2011. Potential bias due to this assumption is discussed in later sections. Sediment and pore-water C concentrations were estimated from Alperin et al. (2000) and Benninger et al. (2008) with the exception of pore-water DOC in the PS, for which no data were available. Degradation of riverine OC to DIC after Irene was quantified by applying a one-dimensional transport model to the freshwater region of the upper estuary, a 54 km^2 region between Sta. 0 and 13 (Fig. 1), where salinity was < 1 on both the 29 August and 08 September P_{CO_2} surveys. Exchange coefficients for DIC, DOC, and POC were determined from 29 August to 08 September using ModMon data and river discharge.

The total DIC contained in NRE waters was quantified based on discrete ModMon samples of surface and bottom water. The pycnocline depth was determined from vertical profiles at each sample station and then spatially interpolated over the NRE surface area in ArcGIS 10.0. Surface- and bottom-water volumes between consecutive stations were calculated using a 2011 bathymetric–topographic digital elevation model (DEM) with 10 m resolution in the NRE-PS (Grothe et al. 2012). DIC concentrations were multiplied by the respective segment volume and summed to give the total DIC. The "exchangeable CO_2," i.e., the quantity of DIC that could be exchanged with the atmosphere before reaching gas-solubility equilibrium, was calculated using CO2SYS (Lewis et al. 1998) and DIC, salinity, temperature, and P_{CO_2} at discrete sample locations.

Current velocities and storm-tide elevation were estimated using several high-resolution data sets: Hurricane Irene storm tides from the Advanced Circulation (ADCIRC) storm surge model and the Simulating Waves Nearshore (SWAN) wind wave model (http://nc-cera.renci.org, Blanton et al. 2012), storm-tide time series from tidal

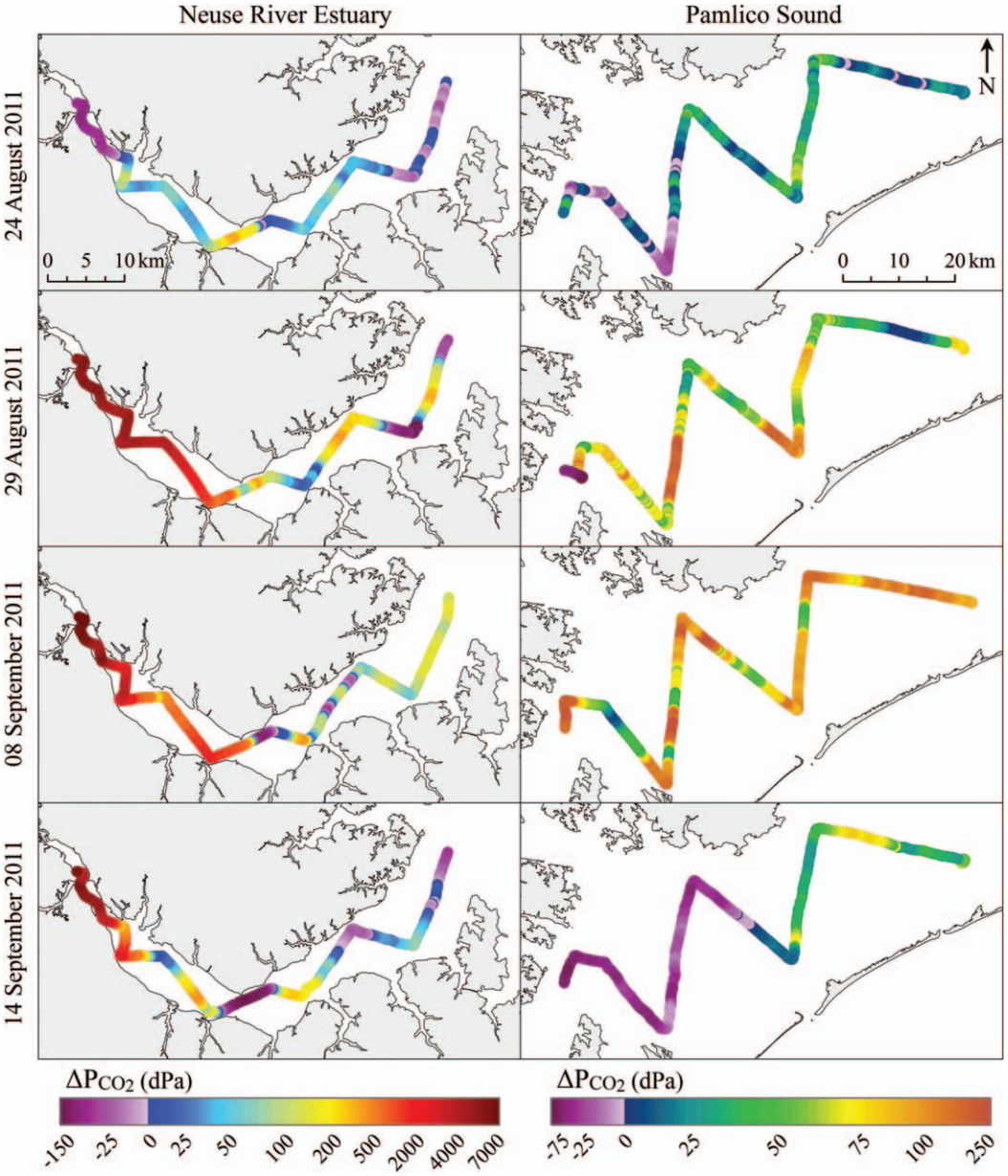

Fig. 3. ΔP_{CO_2} in the NRE and PS 3 d before and 1, 12, and 17 d after Hurricane Irene. Negative values indicate an atmospheric CO_2 sink, while positive values indicate an atmospheric CO_2 source.

gauges in the APS (McCallum et al. 2012), and the aforementioned DEM. The DEM was overlain with storm-tide data in ArcGIS 10.0 to estimate the NRE volume at the maximum and minimum water level. Average current velocities during the flood and ebb storm tides were then determined at the midpoint of the NRE and at the NRE-PS border by dividing the change in NRE volume east of the respective cross section by the average cross-sectional area during the flood and ebb interval.

Results

Hydrographic and hydrological conditions—Prestorm: Three days prior to landfall of Hurricane Irene (24 August), subregions of both the NRE and PS varied from a small CO_2 source to a small CO_2 sink, driven mostly by spatial variations in ΔP_{CO_2} (Fig. 3). No bottom-water P_{CO_2} measurements were collected immediately prior to Irene; however, hydrographic conditions, such as vertical stratification of the water column and hypoxic bottom waters in early August 2011, the latter being a product of intense microbial respiration and production of CO_2, were consistent with previous summertime observations of high P_{CO_2} in subpycnal waters (Table 2). High surface P_{CO_2} was observed on prestorm across-axis surveys during brief upwelling events near Sta. 28. P_{CO_2} in the localized upwelling region exceeded 15,500 dPa on 25 August and 7500 dPa on 26 August, respectively (data not shown), demonstrating the potential exposure of high-P_{CO_2} bottom waters in response to wind-driven forcing.

Table 2. P_{CO_2} survey samples of NRE-PS surface (S) and bottom (B) water.

		July–August 2009				02–24 August 2011						14 September 2011						
	Station	0	13	28	58	0	13	28	58	P2	P4	0	13	28	58	P2	P4	P10	P11	P12
Salinity																				
S		6	11	16	19	7	15	21	24	26	27	1	6	13	16	20	22	21	26	27
B		17	19	21	23	18	21	24	29	27	28	19	21	23	26	27	27	28	28	28
$O_{2(aq)}$ (% sat)																				
S		114	120	110	97	122	114	100	102	102	100	36	108	160	122	125	121	116	109	108
B		11	11	23	16	5	45	27	5	76	68	5	5	6	6	22	53	75	90	91
P_{CO_2} (dPa)																				
S		815	403	398	486	396	386	408	386	409	399	6549	1367	234	393	382	356	391	438	441
B		4057	3598	2294	1855							4122	3314	2339	2167	1374	791	606	530	529

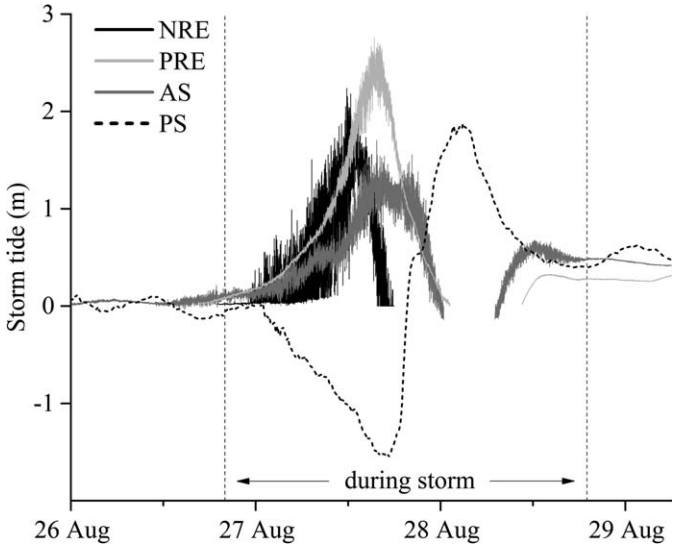

Fig. 4. Storm tide elevation relative to mean surface level in the Neuse River Estuary (NRE), Pamlico River Estuary (PRE), Albemarle Sound (AS), and Pamlico Sound (PS), measured at gauges shown in Fig. 1.

During-storm: The dynamics of the surface P_{CO_2} response to the storm are unknown, but they depend critically on mixing and allochthonous C delivery. For the first 12 h of the storm, northeast winds pushed waters from the PS into the NRE (Figs. 4, 5). The mean depth of the NRE increased from 3.7 m to 5.8 m, more than doubling the NRE volume from 1.7×10^9 m^3 to 4.4×10^9 m^3 (Fig. 6). The mean current velocity required to support this water influx was 1.5 m s^{-1} at Sta. P1 and 2.3 m s^{-1} at Sta. 28. The most-intense physical forcing occurred after Irene's eye passed the NRE, when winds shifted to the west, driving the storm tide back toward the PS (Figs. 4, 5) and decreasing the mean depth of the NRE to approximately 2.7 m in 6 h. Mean current velocities during this interval were 3.0 m s^{-1} at Sta. P1 and 5.0 m s^{-1} at Sta. 28. These wind and current velocities were sufficient to drive strong vertical mixing and sediment resuspension, which would have rapidly increased surface P_{CO_2} at the onset of the storm and maintained vertically constant P_{CO_2} throughout the water column (Luettich et al. 2000; Abril et al. 2010). Based on the aforementioned transport estimates, it appears that the input of C from river discharge and stormwater runoff during Irene was minor relative to wind-driven water displacement (Fig. 6).

Poststorm: On 29 August, the areally averaged P_{CO_2} in the NRE and PS were, respectively, 2000 dPa and 470 dPa, the highest recorded in either system out of 57 surveys between 2009 and 2011 (Figs. 3, 5). The largest pre- to poststorm increase in P_{CO_2} occurred in the upper NRE (Sta. 0-28) and was correlated with a significant increase in NH_4^+ and $NO_3^- + NO_2^-$ (Fig. 3; Table 3). Concentrations of NH_4^+ and $NO_3^- + NO_2^-$ in poststorm Neuse River water were more than 10 times lower than those observed in the upper NRE surface water on 30 August, indicating that the pre- to poststorm increase was primarily due to input from sediment resuspension. The volume-weighted average

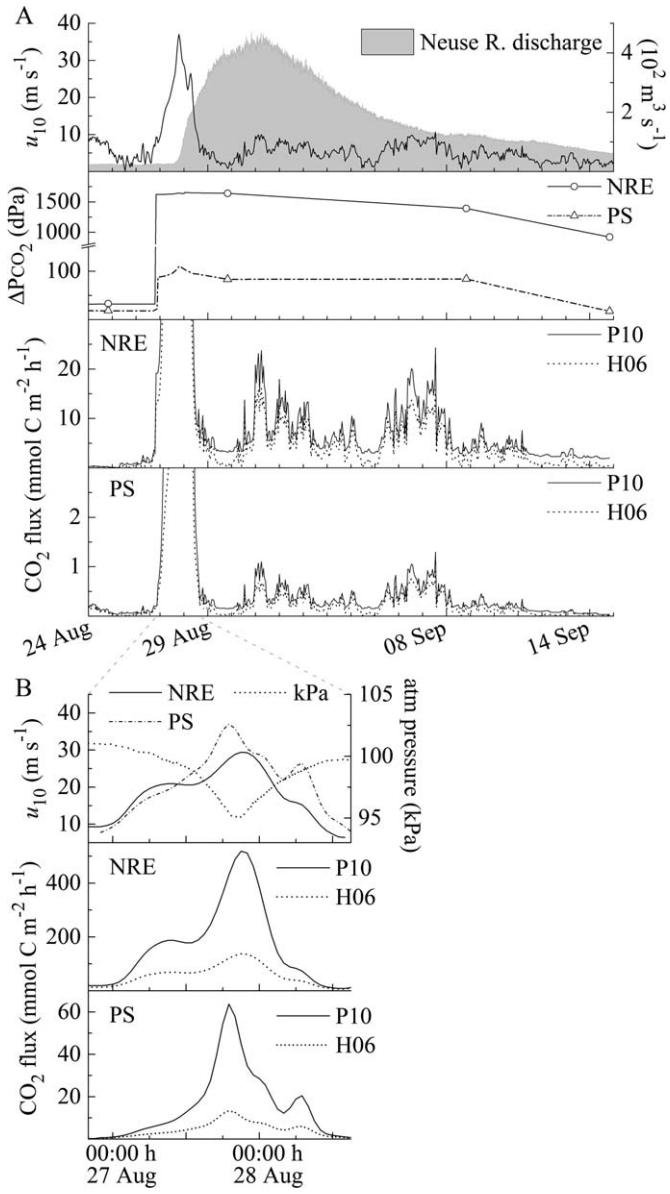

Fig. 5. (A) u_{10}, Neuse River discharge at Ft. Barnwell, North Carolina, ΔP_{CO_2}, and air–water CO_2 flux from 24 August 2011 to 14 September 2011. (B) During-storm u_{10}, atmospheric (atm) pressure, and air–water CO_2 flux.

NH_4^+ on 29–30 August was four times higher than prestorm NH_4^+ in the NRE (Table 3) and two times higher in the PS (data not shown). All prestorm $NO_3^- + NO_2^-$ concentrations in the NRE-PS were below the detection limit of 0.02 μmol N L^{-1}, suggesting that the high P_{CO_2} and $NO_3^- + NO_2^-$ immediately after Irene may be partially due to water-column nitrification during the storm, as discussed in later sections.

The maximum P_{CO_2} occurred near Sta. 0, where values were approximately 7000 dPa on all poststorm surveys (Fig. 3). The high-P_{CO_2} signal rapidly diminished downestuary, as CO_2 was ventilated to the atmosphere, taken up by primary production, or converted to nonvolatile carbonate species (Fig. 3). This trend was consistent with our prior observations in the NRE during flood conditions (Crosswell et al. 2012). Surface-water P_{CO_2} in the lower NRE (Sta. 28-P1) and PS was highly variable, and regions of low P_{CO_2} were strongly correlated with high $O_{2(aq)}$ and Chl *a*. A twofold increase in turbidity after storm passage was observed throughout the NRE-PS (Fig. 7). Some spikes in turbidity were observed near phytoplankton blooms but did not otherwise correlate with Chl *a*. Hence, the high turbidity on 29 August appeared to be due to suspended material that remained in the water column after Irene. Bottom-water data indicate that P_{CO_2} in subpycnal waters increased throughout the poststorm period due to the degradation of OM; poststorm riverine OC concentrations and NH_4^+ in NRE bottom waters were the highest ever recorded by ModMon in the NRE-PS (Table 3).

Hydrologic forcing was the dominant physical control on poststorm P_{CO_2}. Floodwaters delivered high-P_{CO_2}, OM-enriched freshwater to the NRE and drove strong vertical stratification throughout the NRE-PS (Tables 2–4). Storm tide and salinity data show that the NRE-PS quickly restratified late in the during-storm period; as TC-force winds diminished, water from the PS flowed back into APS subestuaries below the less-dense surface water, increasing the water level in NRE, Pamlico River Estuary, and Albemarle Sound (Fig. 4; Tables 3, 4). This strong vertical stratification limited CO_2 exchange between surface and bottom waters throughout most of the NRE-PS. Freshwater input by the poststorm discharge pulse decreased the average surface salinity by ~ 50% (08 September) in the NRE and ~ 15% (14 September) in the PS relative to prestorm conditions (Figs. 5, 7; Tables 3, 4). The response

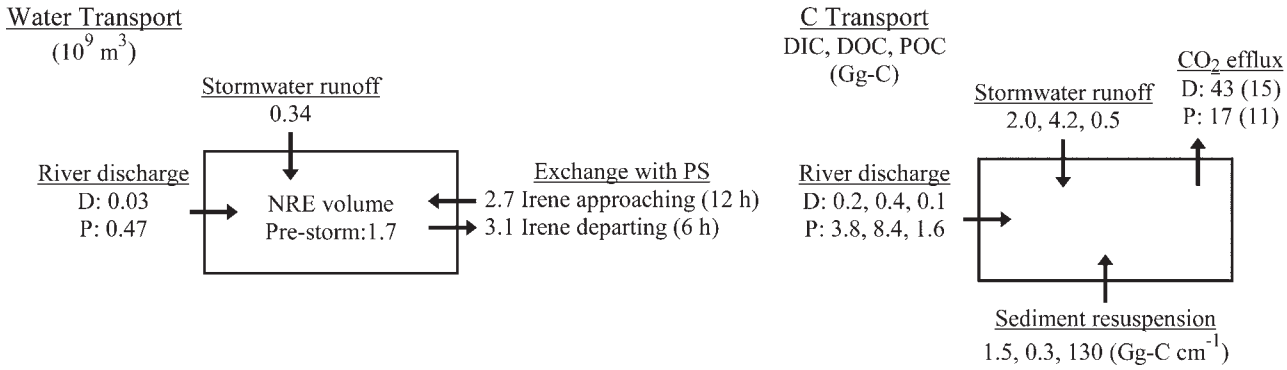

Fig. 6. Water and C budget in the NRE for the during-storm (D) and poststorm (P) periods.

Table 3. ModMon samples of NRE surface (S) and bottom (B) water.

Station	30 August 2011									06 September 2011									19 September 2011								
	0	5	11	13	22	28	35	44	58	0	5	11	13	22	28	35	44	58	0	5	11	13	22	28	35	44	58
Salinity																											
S	0	1	2	3	7	8	18	21	24	0	0	1	1	4	11	12	13	15	4	9	13	14	16	14	18	20	21
B	11	16	18	18	21	22	22	24	25	0	0	13	16	20	22	23	23	25	17	18	14	15	17	20	19	20	21
$O_{2(aq)}$ (% sat)																											
S	21	33	45	44	75	87	88	99	91	5	7	34	35	60	67	81	88	101	50	65	90	88	91	98	100	90	87
B	16	35	36	37	38	41	46	47	53	4	4	19	5	5	58	55	45	74	24	46	83	78	22	73	96	86	84
POC (μmol L^{-1})																											
S	128	96	83	93	70	147	144	213	143	452	421	177	198	127	245	105	115	136	94	120	85	77	99	113	125	100	116
B	130	172	82	98	115	100	131	100	220	449	423	221	319	56	118	197	226	174	94	84	96	74	76	133	149	171	176
DOC (μmol L^{-1})																											
S	1010			864	668	578		391		1842			1482	1169	710		678		1184			821	722	799		511	
B	543			443	372	375		343		1827			549	410	405		385		706			820	624	545		490	
$NO_3^- + NO_2^-$ (μmol L^{-1})*																											
S	3	6	6	7	4	3				1	0	0	0	0				0	8	4	1	1	0	0	0	0	0
B	1	1	1	1	0	0	0	0		0	0								1	0	1	1	0	0	0	0	0
NH_4^+ (μmol L^{-1})																											
S	2	4	5	5	6	4	1	1	1	1	1	6	4	5	1	1	1	2	29	38	27	24	15	22	6	9	12
B	20	13	13	12	10	9	5	2	2	1	1	57	59	11	6	2	2	1	37	26	25	24	18	14	8	11	12

* Blank values were below the detection limit of 0.02 μmol N L^{-1}.

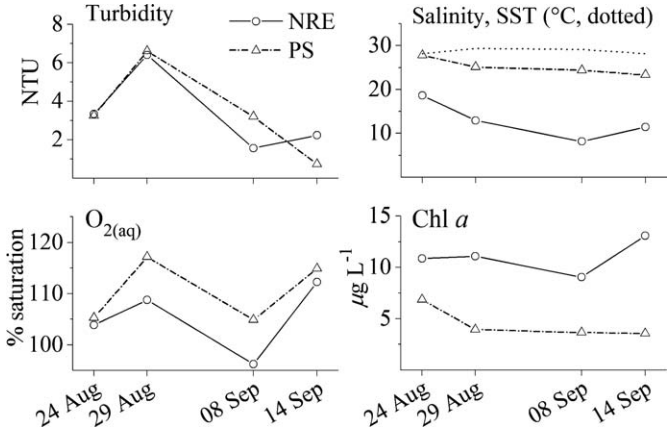

Fig. 7. Areally averaged surface parameters from NRE-PS P_{CO_2} surveys.

time of surface P_{CO_2} to air–water exchange and biological processing was short under these relatively fresh and weakly buffered conditions, contributing to the high spatial and temporal variability observed on poststorm surveys (Fig. 3). Areally averaged surface temperature varied by only 1°C between surveys (Fig. 7) and did not have a significant effect on pre- to poststorm fluxes.

Air–water CO_2 fluxes and C budget—Pre-storm: Areally averaged CO_2 fluxes in the NRE and PS were low immediately prior to Irene. On 24 August, both systems were a CO_2 source of 0.1 (0.1) mmol C m^{-2} h^{-1} (Fig. 5A). On two earlier surveys in August 2011, both systems were small CO_2 sinks. This near-neutral flux from 01 to 24 August was consistent with prior summertime observations in the NRE-PS (Crosswell et al. 2012). By comparison, the NRE and PS were both CO_2 sinks of −0.1 (−0.1) mmol C m^{-2} h^{-1} in August 2010.

During-storm: The average during-storm CO_2 fluxes in the NRE and PS were, respectively, 170 (57) mmol C m^{-2} h^{-1} and 16 (4.6) mmol C m^{-2} h^{-1}, and the maximum fluxes were 520 (140) mmol C m^{-2} h^{-1} and 64 (13) mmol C m^{-2} h^{-1} (Fig. 5B; Table 5). Maximum k values in the NRE and PS were 1030 (270) and 2000 (420) cm h^{-1}, respectively. Regardless of the gas-transfer parameterization, the during-storm fluxes were significant departures from previous fluxes in the NRE-PS (Table 5); the highest CO_2 efflux in the year prior to Irene was 1.4 (0.8) mmol C m^{-2} h^{-1}, and the highest CO_2 uptake was −3.9 (−1.4) mmol C m^{-2} h^{-1}.

The during-storm CO_2 efflux of 43 (15) gigagrams of carbon (Gg-C) from the NRE was not only large relative to nonstorm CO_2 exchange (Table 5), but it was also larger than the capacity of many of the reservoirs and transfers available to support this flux. The prestorm NRE water column contained, at most, 4.4 Gg-C of exchangeable CO_2, even if we assume that the bottom water was characterized by the saline, high-P_{CO_2} waters observed during typical summertime conditions in prior years. Supply of C from river and stormwater runoff during Irene amounted to only 2.2, 4.6, and 0.6 Gg-C as DIC, DOC, and POC, respectively (Fig. 6).

C input from the resuspension of NRE sediment represents the only potential C-supply mechanism that could support the during-storm CO_2 efflux. The estimated DIC, DOC, and POC input per unit depth of sediment resuspension was, respectively, 1.5, 0.3, and 130 Gg-C cm^{-1} depth over the entire NRE (Fig. 6), based on sediment C content from Alperin et al. (2000) and Benninger et al. (2008). The CO_2 efflux of 36 (10) Gg-C from the PS (Table 5) was smaller relative to the DIC and POC input from sediment resuspension: 2.3 and 405 Gg-C cm^{-1} depth, respectively, over the entire PS. Despite this large potential DIC input from sediment resuspension, the DIC : salinity relationship showed a pre- to poststorm decrease throughout the NRE-PS (Fig. 8) and was significantly larger than could be explained by dilution from rainfall, stormwater runoff, or river input (Fig. 6). Hence, this decrease in the DIC : salinity relationship indicates a net loss of DIC from NRE-PS waters during Irene.

Poststorm: The average poststorm CO_2 fluxes in the NRE and PS were 6.4 (4.2) mmol C m^{-2} h^{-1} and 0.3 (0.2) mmol C m^{-2} h^{-1}, respectively (Table 5). Hourly averaged

Table 4. ModMon samples of PS surface (S) and bottom (B) water.

	29 August 2011									08 September 2011								
Station	P1	P2	P3	P4	P5	P6	P7	P8	P9	P1	P2	P3	P4	P5	P6	P7	P8	P9
Salinity																		
S	23	24	23	24	25	25	25	26	25	18	19	21	23	24	24	26	26	19
B	27	26	27	33	33	33	30	28	29	27	26	26	26	29	27	31	27	26
$O_{2(aq)}$ (% sat)																		
S	116	115	112	116	115	113	116	119	109	96	102	108	92	106	108	107	104	100
B	68	72	76	68	78	68	79	80	75	53	79	63	85	70	78	72	92	88
POC (μmol L^{-1})																		
S	393	158	145	121	107	115	113	134	113	185	112	245	109	87	96	93	97	107
B	136	141	131	160	87	80	133	99	113	186	155	131	162	136	132	77	96	132
DOC (μmol L^{-1})																		
S	480	344	353	331	316	316	310	282	344	542	457	433	364	362	335	320	298	456
B	304	329	286	131	128	156	247	281	271	306	291	309	302	239	294	193	284	293

Table 5. Air–water CO_2 flux and total C transport during respective intervals.

	01 Aug 2010–01 Aug 2011		During-storm (42 h)		Poststorm (17 d)	
$k(u_{10})$ equation	(mol C m^{-2} yr^{-1})	(Gg-C)	(mol C m^{-2} h^{-1})	(Gg-C)	(mol C m^{-2} h^{-1})	(Gg-C)
P10 (H06)						
NRE	−16 (−10)	−8.1 (−5.2)	170 (57)	43 (15)	6.4 (4.2)	17 (11)
PS	−15* (−10*)	−22* (−14*)	16 (4.6)	36 (10)	0.3 (0.2)	7.3 (4.5)

* Based on surveys of ~ 33% PS surface area.

u_{10} during this period was approximately equal to the annual average, but poststorm fluxes were significantly higher than prior nonstorm fluxes due to the higher ΔP_{CO_2}. The total poststorm CO_2 efflux was 17 (11) Gg-C from the NRE and 7.3 (4.5) Gg-C from the PS (Table 5).

CO_2 efflux was highest in the river-dominated upper estuary and was larger than could be supported by offgassing of riverine CO_2 alone. We estimated the degradation of OC to DIC in the low-salinity (< 1) region of the upper estuary between 29 August and 08 September, as nonriverine inputs could be considered negligible. CO_2 efflux from the freshwater region was 4.3 (2.9) Gg-C. If exchangeable CO_2 had not been replenished by the degradation of OC during this interval, then the CO_2 efflux could have been, at most, 0.7 Gg-C. Accordingly, degradation of 3.6 Gg-C of OC (35% of the riverine OC input) was required to support the P10-based CO_2 efflux between 29 August and 08 September, while degradation of 2.2 Gg-C of OC (25% of the riverine OC input) was required to support the H06-based CO_2 efflux. Regardless of the gas-transfer parameterization, over 80% of the CO_2 efflux from the freshwater region must have been sustained by degradation of OC.

The lower NRE and PS were net CO_2 sources throughout the poststorm period (Figs. 3, 5), but surface-water P_{CO_2} progressively declined due to CO_2 efflux and isolation of autotrophic surface waters from heterotrophic bottom waters (Tables 3, 4). Strong vertical stratification allowed large regions of the NRE and western PS to function as sinks for atmospheric CO_2 by 14 September, while the relatively well-mixed eastern PS remained an atmospheric CO_2 source (Fig. 3; Table 2). We estimate that NRE-PS surface waters on 14 September contained 6 Gg-C of exchangeable CO_2; however, a large quantity of exchangeable CO_2 (~ 60 Gg-C) remained stored in subpycnal waters due to the widespread vertical stratification sustained by the poststorm freshwater discharge pulse.

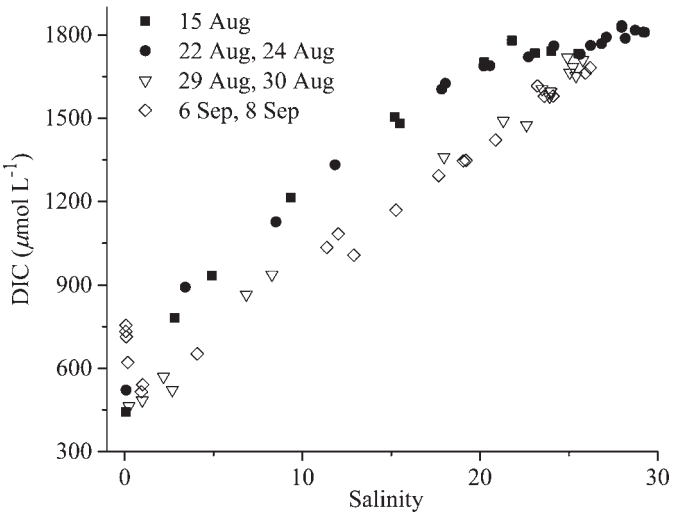

Fig. 8. DIC : salinity relationship in the NRE (15 August, 24 August, 30 August, 06 September) and PS (22 August, 29 August, 08 September) surface water.

Effect of Hurricane Irene on the annual C budget—In the year prior to Irene, areally averaged P_{CO_2} in the NRE and PS ranged from 270 to 480 dPa (15 surveys) and 350 to 430 dPa (8 surveys), respectively, and both systems functioned as annual sinks for atmospheric CO_2 (Table 5). From 01 August 2010 to 01 August 2011, the atmospheric C input of −8.1 (−5.2) Gg-C to the NRE equaled ~ 25% of the annual riverine C input: 11, 14, and 1.0 Gg-C as DIC, DOC, and POC, respectively.

On the three poststorm surveys, areally averaged P_{CO_2} was 2000, 1500, and 1100 dPa in the NRE and 470, 450, and 410 dPa in the PS. The CO_2 efflux from the NRE over the 20 d during- and poststorm study period was 61 (26) Gg-C, a source with magnitude over seven (five) times greater than the nonstorm annual CO_2 uptake of −8.1 (−5.2) Gg-C (Table 5). Despite the much larger area of the PS, the 20 d CO_2 efflux (43 [15] Gg-C) was lower than the NRE efflux and offset a relatively smaller portion of the annual CO_2 uptake. Riverine and stormwater C input to the NRE over the 20 d study period was 6.0, 13, and 2.2 Gg-C as DIC, DOC, and POC, respectively, and was comparable to the annual Neuse River C input prior to Irene (Fig. 6).

Discussion

Controls on during-storm fluxes—Surface P_{CO_2}: The stepwise interpolation of during-storm P_{CO_2} had a significant effect on CO_2 flux estimates, and this choice requires justification for the response of a relatively fresh, shallow estuary to an extreme wind event like Irene. Given the elevated P_{CO_2} in bottom waters, we can reasonably assume that a steep increase in P_{CO_2} occurred as the NRE-PS water column was completely mixed early in the during-storm period (Abril et al. 2010). After this initial mixing, it might be expected that P_{CO_2} in the weakly buffered waters of the NRE-PS would rapidly approach gas-solubility equilibrium due to the exponential increase in gas-transfer velocity. However, the pre- to poststorm P_{CO_2} response was not toward equilibrium, but rather showed a significant

increase in P_{CO_2} across the entire system. For surface P_{CO_2} to remain above atmospheric P_{CO_2} during the storm, the air–water CO_2 efflux must have been partially balanced by CO_2 input to the water column. The degree to which surface P_{CO_2} initially increased and subsequently decreased during the storm cannot be determined given the multiple drivers of the P_{CO_2} dynamics. As a conservative estimate, we assume that the lowest possible P_{CO_2} after initial mixing, the average surface P_{CO_2} on 29 August, was relatively constant throughout the storm. Supporting this assumption, Evans et al. (2012) found that surface-water P_{CO_2} in the Columbia River Estuary, Oregon–Washington, U.S.A., decreased after a major storm and was lowest ~1 d after high winds diminished.

It is possible that metabolic processes may have influenced P_{CO_2} prior to the first poststorm survey on 29 August. However, $O_{2(aq)}$ on 29 August was above atmospheric equilibrium (Fig. 7), indicating that the pre- to poststorm P_{CO_2} increase occurred during the storm. If P_{CO_2} had increased immediately after the storm due to persistent oxidation of resuspended material, a subsaturated $O_{2(aq)}$ signature would have been retained under the low-wind conditions (Fig. 5A). Instead, the high $O_{2(aq)}$ on 29 August indicated that P_{CO_2} in the 24 h period after the storm would have decreased due to metabolic CO_2 uptake. Supersaturation of surface $O_{2(aq)}$ can also occur due to bubble entrainment at high wind speeds, but areally averaged $O_{2(aq)}$ on 29 August (145% in the lower NRE, 117% in the PS) was significantly higher than could be explained by bubble entrainment alone and required $O_{2(aq)}$ input from autotrophic production (McNeil and D'Asaro 2007). While it is apparent that oxidation of resuspended material increased P_{CO_2} during the storm, as discussed in the following section, this low-$O_{2(aq)}$ signature would have been lost due to the high gas-transfer velocity of O_2.

Replenishment of surface P_{CO_2}: River and stormwater DIC input during Irene was < 15% of the during-storm CO_2 efflux from the NRE. This may be an underestimate due to our assumption that freshwater C content during the storm was equal to the freshwater sample collected on 30 August. Yoon and Raymond (2012) showed that stormwater DOC concentrations in an Irene-affected watershed rapidly increased at the onset of the storm but had decreased by 60% 2 d after storm passage. If stormwater C concentrations were also 60% higher in the NRE, then the during-storm freshwater input for DIC, DOC, and POC would equal 4.4, 9.2, and 1.2 Gg-C, respectively. Applying these higher loading values and assuming one third of this OC was labile, as observed by Yoon and Raymond (2012), we estimate that freshwater inputs could replenish, at most, 7.9 Gg-C of the during-storm CO_2 efflux from the NRE (43 [15] Gg-C). Even using this upper bound for freshwater input, a much larger DIC input from sediment resuspension is required to account for the pre- to poststorm increase in surface P_{CO_2}.

In estuaries like the NRE-PS, high wind speeds increase air–water CO_2 efflux but also increase wave action and current velocities, which resuspend sediments (Luettich et al. 2000; Whipple et al. 2006). By this mechanism, the input of DIC from pore waters could actively replenish a portion of the CO_2 lost to air–water efflux during the storm. Benninger et al. (2008) observed a sediment resuspension depth of > 24 cm from even the deepest regions of the NRE-PS during Hurricane Floyd (1999), a similarly large but less-intense TC than Irene. If we assume the same resuspension depth during Irene, then the mobilization of DIC, DOC, and POC into the NRE water column would equal 35, 7.2, and 3200 Gg-C, respectively, and mobilization of DIC and POC into the PS water column would equal 56 and 9800 Gg-C, respectively. The pre- to poststorm decrease in DIC : salinity (Fig. 8) indicates that this large input of pore-water DIC must have been coupled with a reduction in water-column pH.

Exposure of anoxic estuarine sediment and pore water to oxic conditions, e.g., during TC-driven resuspension, can rapidly increase water-column DIC and decrease pH due to oxidation of OM and reduced inorganic compounds (Eggleton and Thomas 2004; Middelburg and Herman 2007; Abril et al. 2010). Abril et al. (2010) found that the most significant changes in DIC and pH of in vitro sediment resuspensions occurred within 24 h of resuspension, and the authors estimated a conservative OM oxidation rate of 0.6 mol C m^{-3} d^{-1}. If we apply this rate to the average NRE volume (2.5×10^9 m^3) during the 43 h during-storm period, then 18 Gg-C of resuspended OM would be oxidized to DIC, accounting for 40% of the P10-based during-storm CO_2 efflux from the NRE. Autotrophic oxidation also appeared to have a significant effect on during-storm CO_2 efflux. If we assume that all poststorm $NO_3^- + NO_2^-$ was produced by particle-associated bacteria that were resuspended during the storm, then water-column nitrification alone would decrease pH in the upper NRE by 0.1. The corresponding P_{CO_2} increase would account for 25% of the during-storm CO_2 efflux from the entire NRE. The decrease in pH due to other biological and chemical oxidation of resuspended inorganic material during Irene cannot be determined; however, prior research has shown that NRE sediments contain high concentrations of reduced inorganic compounds (Matson et al. 1983). Thus, it seems plausible that oxidation of resuspended inorganic compounds, input of pore-water DIC, and high gas-transfer velocities could account for the remaining 35% of the P10-based during-storm CO_2 efflux and the pre- to poststorm decrease in DIC : salinity.

Controls on poststorm fluxes—Biological processing: Degradation of riverine OC input was the dominant driver of CO_2 efflux from the upper NRE, based on mass-flux estimates between 29 August and 08 September. These results are consistent with observations from other Irene-affected regions of the Mid-Atlantic Coast. Yoon and Raymond (2012) and Dhillon and Inamdar (2013) showed that the erosive energy of Irene's extreme winds and rainfall mobilized labile OC that would otherwise remain in terrestrial sediments, and Klug et al. (2012) found that this high OC loading dramatically increased heterotrophic respiration in Irene-affected lakes.

The contribution of riverborne OM decreased along the longitudinal axis of the NRE and had a relatively smaller effect on surface waters of the lower NRE and PS, where

primary production increased, and poststorm CO_2 efflux appeared to be driven by nonriverine sources. For example, a large phytoplankton bloom and low P_{CO_2} were noted on 29 August between Sta. 58 and P1, which is bordered by 200 km^2 of farmland that was inundated by storm tides (Figs. 1, 3). Patchy phytoplankton blooms were similarly observed after Hurricane Floyd, where Paerl et al. (2001) and Tester et al. (2003) found that high Chl *a* in the lower NRE and PS was driven by the input of inorganic nutrients scoured from marshes and swamps by storm tides. Supersaturation of both CO_2 and $O_{2(aq)}$ in the lower NRE and PS after Irene, along with the prior observations of Paerl et al. (2001) and Tester et al. (2003), indicates that TC-driven export of nutrients and DIC from estuary sediments and surrounding wetlands can support net efflux of CO_2 to the atmosphere even in net autotrophic surface waters.

Hydrological forcing: Water-column stratification driven by river discharge was a major control on poststorm CO_2 fluxes in the NRE-PS. Enhanced primary production decreased surface P_{CO_2} over the poststorm period, while the degradation of OM increased the quantity of exchangeable CO_2 stored in subpycnal waters by a factor of 10 relative to prestorm conditions (Tables 2–4). We expect that this is a characteristic response of large, shallow estuaries like the APS to similar major storm events, but the magnitude and duration of hydrological forcing can vary depending on TC intensity and the frequency of subsequent TCs. For example, three consecutive TCs in 1999 (Dennis, Floyd, and Irene) and a more-intense, longer-duration TC in 1996 (Fran) vertically stratified the entire NRE-PS for months rather than weeks (Paerl et al. 2001). Hence, it is clear that the degree of physical and biogeochemical perturbation of coastal waters depends on the frequency, intensity, duration, and other storm-specific attributes of TCs (Wetz and Yoskowitz 2013). A quantitative assessment of the ways in which air–water CO_2 efflux may vary among different TC scenarios requires further research with longer poststorm observation periods and emphasis on the persistence of C reservoirs that could support air–water CO_2 efflux.

The future of coastal C storage—Effects of TCs on regional C budgets: There is compelling evidence that macrotidal, well-mixed estuaries are sources of atmospheric CO_2 due to the degradation of allochthonous OM, but few microtidal estuaries have been studied with regard to CO_2 flux (Borges and Abril 2011; Crosswell et al. 2012). The annual CO_2 uptakes for the NRE and PS prior to Irene (Table 5) were larger per area than previously observed in any estuary (Laruelle et al. 2013), supporting the growing body of evidence that microtidal systems can be significant CO_2 sinks in the absence of TC-driven perturbation (Koné et al. 2009; Crosswell et al. 2012; Maher and Eyre 2012). Microtidal, wind-driven estuaries represent $> 70\%$ of the estuarine surface area along the U.S. Atlantic and Gulf Coasts (43,607 km^2 microtidal, 18,363 km^2 macrotidal; NOAA Coastal Assessment Framework), and it is reasonable to hypothesize that perturbation by TCs can dramatically increase CO_2 efflux from these estuaries and, in some cases, like the NRE-PS, can convert these systems from annual sinks to annual sources for atmospheric CO_2.

We are confident that our results scale up to the greater APS system due to the similar watershed, hydrology, and sediment characteristics of the Pamlico River Estuary and Albemarle Sound to the NRE (Matson et al. 1983; Fig. 1). A preliminary budget over this area, as described in the Methods, shows an air–water efflux of 610 (240) Gg-C during the 20 d study period. The APS system represents $< 25\%$ of the estuary surface area in the continental U.S. that experienced extreme winds and storm tides during Irene, and it is likely that the other Irene-affected estuaries experienced a similar increase in air–water CO_2 efflux. Supporting this, biogeochemical and hydrological effects observed after prior TCs in U.S. Atlantic and Gulf Coast estuaries (e.g., during-storm sediment resuspension and ventilation of bottom waters, and enhanced poststorm OM loading, primary production, and bottom-water hypoxia) were similar to those observed in the NRE-PS after Irene (Nichols 1993; Hagy et al. 2006; Wetz and Yoskowitz 2013). If we scale our results to all estuaries in the path of Irene, then we estimate a regional CO_2 emission of 3 (1) Tg-C due to Hurricane Irene. This efflux is of comparable magnitude to recent estimates of the global TC-driven CO_2 efflux from oceans (7 Tg-C yr^{-1}; Lévy et al. 2012), suggesting that TC-driven CO_2 efflux from coastal waters may be an important component of large-scale C budgets.

C pool reactivity: During periods of low TC activity, organic and inorganic C is thought to be conserved within the APS system due to efficient biogeochemical recycling and low-energy conditions (Matson et al. 1983). Our results show that perturbation by TCs can lead to large export of C to the atmosphere, supported mostly by mobilization of pore-water DIC and oxidation of sediment-bound OC. A corollary to this scenario is that while a TC may remove C from estuary sediments, the same TC could rapidly replenish sediment and pore-water C stocks via allochthonous inputs and stimulation of autochthonous C production and processing in systems undergoing rapid eutrophication (Paerl et al. 2006; Middelburg and Herman 2007). However, based on the poststorm and annual C input to the NRE, it would take at least two nonstorm years to replenish the sediment C stocks, even if all allochthonous and autochthonous OC were retained within the NRE.

Hurricane Irene was a low-intensity TC that predominantly affected the coastal APS watershed. More-intense or more-frequent TCs can lead to much higher OC loading to estuaries (Wetz and Yoskowitz 2013). Benninger et al. (2008) showed that that the large export of planktonic OC from PS sediments due to three sequential hurricanes in 1999 was balanced by the input of terrestrial OC. Similarly, Chambers et al. (2007) estimated that Hurricane Katrina (category 3 at landfall) mobilized 105 Tg of biomass-derived C from U.S. Gulf Coast forests, and the results of Yoon and Raymond (2012) and Dhillon and Inamdar (2013) suggest that ensuing hurricanes (Hurricanes Rita 2005, Gustav 2008, and Ike 2008) could have washed much of this OC into estuaries along the U.S. Gulf Coast (e.g., Barataria Bay, Mobile Bay, and Lake Pontchartrain). These and other broadly distributed microtidal estuaries

are similar to the APS (Reynolds-Fleming and Luettich 2004; Kennish and Paerl 2010), and the capacity of these estuaries to preserve OC in coastal sediments is expected to diminish due to anthropogenic changes in land use and drainage-network hydrology combined with rising sea levels and increased TC activity (Moorhead and Brinson 1995; Culver et al. 2007). More frequent cycles of OC deposition and resuspension in shallow coastal waters can lead to progressive photo- and microbial decay, and the cumulative effect of these processes provides a mechanism whereby even refractory OC can be degraded to DIC (Mayer et al. 2006). Although TC-driven CO_2 efflux from estuaries may be partially balanced by the input of terrestrial OM, the translocation of C from long-term reservoirs to estuary sediments represents a pathway toward export to the atmosphere or ocean.

Response to changing TC activity: Globally, coastal ecosystems play a significant role in C sequestration and long-term storage, but changing TC activity may alter the storage capacity of coastal C reservoirs (Hopkinson et al. 2008; Morton and Barras 2011; Wetz and Yoskowitz 2013). TCs directly affect the fate of C stocks by exposing C that was previously nonvolatile or resistant to decay (e.g., biologically fixed, loosely bound to mineral surfaces, or stored in anoxic environments) to conditions that favor C remineralization and drive CO_2 emissions (Blair and Aller 2012). Anecdotal evidence suggests that more severe storms mobilize a greater proportion of these C stocks than lesser storms; TCs of category 3 or higher have been shown to mobilize C that has accumulated in terrestrial and coastal C reservoirs over decades or even centuries (Chambers et al. 2007; Morton and Barras 2011; DeLaune and White 2012). If the projected shift toward higher-intensity storms releases more C than can be replenished despite an overall decrease in TC frequency, long-term C storage in coastal regions will ultimately be reduced, displacing C to the atmospheric and oceanic reservoirs.

Regional projection of these altered coastal C sources and sinks remains uncertain due to both the poor downscaling capabilities of global climate models (IPCC 2013) and the lack of quantification of contemporaneous C budgets and processes involved. Results presented here represent an important first step toward quantifying the effect of TC on coastal C dynamics, indicating that a substantial amount of C mobilized by a single, relatively low-intensity TC is released to the atmosphere in coastal waters rather than simply relocated from terrestrial and wetland storage to an oceanic C sink.

Acknowledgments

We thank the technicians in the Paerl Laboratory at the University of North Carolina at Chapel Hill, Institute of Marine Sciences, who helped with sample collection and analysis. We also thank two anonymous reviewers, whose insightful comments have helped improve this manuscript. This work was supported by a National Science Foundation Chemical Oceanography grant (Ocean Sciences 0726989) to H.W. Paerl., M.S. Wetz, and B. Hales. Monitoring samples were collected by the Neuse River Estuary Modeling and Monitoring Project (ModMon), supported by the North Carolina Department of Environment and Natural Resources and the Lower Neuse Basin Association and Neuse River Compliance Association.

References

Abril, G., M. Commarieu, H. Etcheber, J. Deborde, B. Deflandre, M. K. Zivadinovic, G. Chaillou, and P. Anschutz. 2010. In vitro simulation of oxic/suboxic diagenesis in an estuarine fluid mud subjected to redox oscillations. Estuar. Coast. Shelf Sci. **88:** 279–291, doi:10.1016/j.ecss.2010.04.003

———, ———, A. Sottolichio, P. Bretel, and F. Guerin. 2009. Turbidity limits gas exchange in a large macrotidal estuary. Estuar. Coast. Shelf Sci. **83:** 342–348, doi:10.1016/j.ecss.2009.03.006

Alin, S. R., F. Maria de Fátima, C. I. Salimon, J. E. Richey, G. W. Holtgrieve, A. V. Krusche, and A. Snidvongs. 2011. Physical controls on carbon dioxide transfer velocity and flux in low-gradient river systems and implications for regional carbon budgets. J. Geophys. Res. **116:** G01009, doi:10.1029/2010JG001398

Alperin, M., E. Clesceri, J. Wells, D. Albert, J. McNinch, and C. Martens. 2000. Sedimentary processes and benthic–pelagic coupling, p. 63–105. *In* Neuse River Estuary Modeling and Monitoring Project Final Report: UNC-WRRI-2000-325B. Water Resources Research Institute, North Carolina State Univ.

Bauer, J. E., W. Cai, P. A. Raymond, T. S. Bianchi, C. S. Hopkinson, and P. A. Regnier. 2013. The changing carbon cycle of the coastal ocean. Nature **504:** 61–70, doi:10.1038/nature12857

Benninger, L. K., M. J. Alperin, J. T. Wells, B. J. Ream, P. Muñoz, Y. Nie, B. Mislowack, and S. Lafond. 2008. Impact of Hurricane Floyd on sediment deposition, erosion, and benthic nutrient fluxes in Pamlico Sound, North Carolina. Report No. 364. Water Resources Research Institute, Univ. North Carolina.

Blair, N. E., and R. C. Aller. 2012. The fate of terrestrial organic carbon in the marine environment. Annu. Rev. Mar. Sci. **4:** 401–423, doi:10.1146/annurev-marine-120709-142717

Blanton, B., J. McGee, J. Fleming, C. Kaiser, H. Kaiser, H. Lander, R. Luettich, K. Dresback, and R. Kolar. 2012. Urgent computing of storm surge for North Carolina's coast. Proc. Comp. Sci. **9:** 1677–1686, doi:10.1016/j.procs.2012.04.185

Borges, A. V., and G. Abril. 2011. Carbon dioxide and methane dynamics in estuaries, p. 119–161. *In* E. Wolanski and D. McLusky [eds.], Treatise on estuarine and coastal science, Volume 5: Biogeochemistry. Academic Press.

———, B. Delille, L.-S. Schiettecatte, F. Gazeau, G. Abril, and M. Frankignoulle. 2004. Gas transfer velocities of CO_2 in three European estuaries (Randers Fjord, Scheldt and Thames), Limnol. Oceanogr. **49:** 1630–1641.

Brown, M. M., R. P. Mulligan, and R. L. Miller. 2014. Modeling the transport of freshwater and dissolved organic carbon in the Neuse River Estuary, NC, USA, following Hurricane Irene (2011). Estuar. Coast. Shelf Sci. **139:** 148–158, doi:10.1016/j.ecss.2014.01.005

Chambers, J. Q., J. I. Fisher, H. Zeng, E. L. Chapman, D. B. Baker, and G. C. Hurtt. 2007. Hurricane Katrina's carbon footprint on US Gulf Coast forests. Science **318:** 1107–1107, doi:10.1126/science.1148913

Crosswell, J. R., M. S. Wetz, B. Hales, and H. W. Paerl. 2012. Air–water CO_2 fluxes in the microtidal Neuse River Estuary, North Carolina. J. Geophys. Res. **117:** C08017, doi:10.1029/2012JC007925

Culver, S. J., C. G. Pre, D. J. Mallinson, S. R. Riggs, D. R. Corbett, J. Foley, M. Hale, L. Metger, J. Ricardo, and J. Rosenberger. 2007. Late Holocene barrier island collapse: Outer Banks, North Carolina, USA. Sediment. Rec. **5:** 4–8.

DeLaune, R., and J. White. 2012. Will coastal wetlands continue to sequester carbon in response to an increase in global sea level?: A case study of the rapidly subsiding Mississippi River deltaic plain. Clim. Change **110:** 297–314, doi:10.1007/s10584-011-0089-6

Dhillon, G. S., and S. Inamdar. 2013. Extreme storms and changes in particulate and dissolved organic carbon in runoff: Entering uncharted waters? Geophys. Res. Lett. **40:** 1322–1327, doi:10.1002/grl.50306

Duarte, C. M., J. Middelburg, and N. Caraco. 2005. Major role of marine vegetation on the oceanic carbon cycle. Biogeosciences **2:** 1–8. doi:10.5194/bg-2-1-2005

Edson, J., C. Fairall, L. Bariteau, C. Zappa, A. Cifuentes-Lorenzen, W. McGillis, S. Pezoa, J. Hare, and D. Helmig. 2011. Direct covariance measurement of CO_2 gas transfer velocity during the 2008 Southern Ocean Gas Exchange Experiment: Wind speed dependency. J. Geophys. Res. **116:** C00F10, doi:10.1029/2011JC007022

Eggleton, J., and K. V. Thomas. 2004. A review of factors affecting the release and bioavailability of contaminants during sediment disturbance events. Environ. Int. **30:** 973–980, doi:10.1016/j.envint.2004.03.001

Evans, W., B. Hales, and P. G. Strutton. 2012. PCO_2 distributions and air–water CO_2 fluxes in the Columbia River estuary. Estuar. Coast. Shelf Sci. **117:** 260–272, doi:10.1016/j.ecss.2012.12.003

Grothe, P. R., L. A. Taylor, B. W. Eakins, K. S. Carignan, M. R. Love, E. Lim, and D. Z. Friday. 2012. Digital elevation models of Morehead City, North Carolina: Procedures, data sources and analysis. NOAA Technical Memorandum NESDIS NGDC-64. U.S. Dept. of Commerce.

Ha, H. K., and K. Park. 2012. High-resolution comparison of sediment dynamics under different forcing conditions in the bottom boundary layer of a shallow, micro-tidal estuary. J. Geophys. Res. **117:** C06020, doi:10.1029/2012JC007878

Hagy, J. D., J. C. Lehrter, and M. C. Murrell. 2006. Effects of Hurricane Ivan on water quality in Pensacola Bay, Florida. Estuar. Coast. **29:** 919–925.

Ho, D. T., S. Ferrón, V. C. Engel, L. G. Larsen, and J. G. Barr. 2014. Air–water gas exchange and CO_2 flux in a mangrove-dominated estuary. Geophys. Res. Lett. **41:** 1–6, doi:10.1002/2013GL058748

———, C. S. Law, M. J. Smith, P. Schlosser, M. Harvey, and P. Hill. 2006. Measurements of air–sea gas exchange at high wind speeds in the Southern Ocean: Implications for global parameterizations. Geophys. Res. Lett. **33:** L16611, doi:10.1029/2006GL026817

———, P. Schlosser, and P. M. Orton. 2011. On factors controlling air–water gas exchange in a large tidal river. Estuar. Coast. **34:** 1103–1116, doi:10.1007/s12237-011-9396-4

Hopkinson, C. S., A. E. Lugo, M. Alber, A. P. Covich, and S. J. Van Bloem. 2008. Forecasting effects of sea-level rise and windstorms on coastal and inland ecosystems. Front. Ecol. Environ. **6:** 255–263, doi:10.1890/070153

Huang, P., and J. Imberger. 2010. Variation of pCO_2 in ocean surface water in response to the passage of a hurricane. J. Geophys. Res. **115:** C10024, doi:10.1029/2010JC006185

Intergovernmental Panel on Climate Change (IPCC). 2013. Climate change 2013: The physical science basis. Working Group I contribution to the IPCC Fifth Assessment Report (AR5). IPCC.

Jiang, L. Q., W. J. Cai, and Y. Wang. 2008. A comparative study of carbon dioxide degassing in river- and marine-dominated estuaries. Limnol. Oceanogr. **53:** 2603–2615, doi:10.4319/lo.2008.53.6.2603

Kennish, M. J., and H. W. Paerl. 2010. Coastal lagoons: Critical habitats of environmental change. CRC Press.

Klug, J. L. D. C. Richardson, H. A. Ewing, B. R. Hargreaves, N. R. Samal, D. Vachon, D. C. Pierson, A. M. Lindsey, D. M. O'Donnell, S. W. Effler, and K. C. Weathers. 2012. Ecosystem effects of a tropical cyclone on a network of lakes in northeastern North America. Environ. Sci. Technol. **46:** 11693–11701, doi:10.1021/es302063v

Koné, Y. J. M., G. Abril, K. N. Kouadio, B. Delille, and A. V. Borges. 2009. Seasonal variability of carbon dioxide in the rivers and lagoons of Ivory Coast (West Africa). Estuar. Coast. **32:** 246–260, doi:10.1007/s12237-008-9121-0

Laruelle, G., H. Dürr, R. Lauerwald, J. Hartmann, C. Slomp, N. Goossens, and P. Regnier. 2013. Global multi-scale segmentation of continental and coastal waters from the watersheds to the continental margins. Hydrol. Earth Syst. Sci. **17:** 2029–2051, doi:10.5194/hess-17-2029-2013

Lévy, M., M. Lengaigne, L. Bopp, E. M. Vincent, G. Madec, C. Ethé, D. Kumar, and V.V.S.S. Sarma. 2012. Contribution of tropical cyclones to the air–sea CO_2 flux: A global view. Glob. Biogeochem. Cy. **26:** GB2001, doi:10.1029/2011GB004145

Lewis, E., D. Wallace, and L. J. Allison. 1998. Program developed for CO_2 system calculations. Carbon Dioxide Information Analysis Center.

Luettich, R. A., J. E. McNinch, H. W. Paerl, C. H. Peterson, J. T. Wells, M. Alperin, C. S. Martens, and J. L. Pinckney. 2000. Neuse River Estuary Modeling and Monitoring Project stage 1: Hydrography and circulation, water column nutrients and productivity, sedimentary processes and benthic–pelagic coupling, and benthic ecology. UNC-WRRI-2000-325B. Water Resources Research Institute, North Carolina State Univ.

Maher, D. T., and B. D. Eyre. 2012. Carbon budgets for three autotrophic Australian estuaries: Implications for global estimates of the coastal air–water CO_2 flux. Global Biogeochem. Cy. **26:** GB1032, doi:10.1029/2011GB004075

Marino, R., and R. W. Howarth. 1993. Atmospheric oxygen exchange in the Hudson River: Dome measurements and comparison with other natural waters. Estuaries **16:** 433–445, doi:10.2307/1352591

Matson, E. A., M. M. Brinson, D. D. Cahoon, and G. J. Davis. 1983. Biogeochemistry of the sediments of the Pamlico and Neuse River estuaries, North Carolina. UNC-WRRI-83-191. Water Resources Research Institute, North Carolina State Univ.

Mayer, L. M., L. L. Schick, K. Skorko, and E. Boss. 2006. Photodissolution of particulate organic matter from sediments. Limnol. Oceanogr. **51:** 1064–1071, doi:10.4319/lo.2006.51.2.1064

McCallum, B. E., Painter, J. A., and E. R. Frantz. 2012. Monitoring inland storm tide and flooding from Hurricane Irene along the Atlantic Coast of the United States, August 2011 [Internet]. U.S. Geological Survey Open-File Report 2012 [accessed 01 April 2013]. Available from http://pubs.usgs.gov/of/2012/1022/

McGillis, W. R., J. B. Edson, J. D. Ware, J. W. Dacey, J. E. Hare, C. W. Fairall, and R. Wanninkhof. 2001. Carbon dioxide flux techniques performed during GasEx-98. Mar. Chem. **75:** 267–280, doi:10.1016/S0304-4203(01)00042-1

McNeil, C., and E. D'Asaro. 2007. Parameterization of air–sea gas fluxes at extreme wind speeds. J. Mar. Syst. **66:** 110–121, doi:10.1016/j.jmarsys.2006.05.013

Middelburg, J. J., and P. M. Herman. 2007. Organic matter processing in tidal estuaries. Mar. Chem. **106:** 127–147, doi:10.1016/j.marchem.2006.02.007

Moorhead, K. K., and M. M. Brinson. 1995. Response of wetlands to rising sea level in the lower coastal plain of North Carolina. Ecol. Appl. **5:** 61–271, doi:10.2307/1942068

Morton, R. A., and J. A. Barras. 2011. Hurricane impacts on coastal wetlands: A half-century record of storm-generated features from southern Louisiana. J. Coast. Res. **27:** 27–43, doi:10.2112/JCOASTRES-D-10-00185.1

Nichols, M. M. 1993. Response of coastal plain estuaries to episodic events in the Chesapeake Bay region. Coast. Estuar. Stud. **42:** 1–20. doi:10.1029/CE042p0001

Paerl, H. W., J. D. Bales, L. W. Ausley, C. P. Buzzelli, L. B. Crowder, L. A. Eby, J. M. Fear, M. Go, B. L. Peierls, and T. L. Richardson. 2001. Ecosystem impacts of three sequential hurricanes (Dennis, Floyd, and Irene) on the United States' largest lagoonal estuary, Pamlico Sound, NC. Proc. Acad. Natl. Sci. USA **98:** 5655–5660, doi:10.1073/pnas.101097398

———, L. M. Valdes, B. L. Peierls, J. E. Adolf, and L. W. Harding, Jr. 2006. Anthropogenic and climatic influences on the eutrophication of large estuarine ecosystems. Limnol. Oceanogr. **51:** 448–462, doi:10.4319/lo.2006.51.1_part_2.0448

Prytherch, J., M. J. Yelland, R. W. Pascal, B. I. Moat, I. Skjelvan, and M. A. Srokosz. 2010. Open ocean gas transfer velocity derived from long-term direct measurements of the CO_2 flux. Geophys. Res. Lett. **37:** L23607, doi:10.1029/2010GL045597

Raymond, P. A., and J. J. Cole. 2001. Gas exchange in rivers and estuaries: Choosing a gas transfer velocity. Estuaries **24:** 312–317, doi:10.2307/1352954

Regnier, P., P. Friedlingstein, P. Ciais, F. T. Mackenzie, N. Gruber, I. A. Janssens, G. G. Laruelle, R. Lauerwald, S. Luyssaert, and A. J. Andersson. 2013. Anthropogenic perturbation of the carbon fluxes from land to ocean. Nat. Geosci. **6:** 596–607, doi:10.1038/ngeo1830

Reynolds-Fleming, J. V., and R. A. Luettich. 2004. Wind-driven lateral variability in a partially mixed estuary. Estuar. Coast. Shelf Sci. **60:** 395–407, doi:10.1016/j.ecss.2004.02.003

Sampere, T. P., T. S. Bianchi, S. G. Wakeham, and M. A. Allison. 2008. Sources of organic matter in surface sediments of the Louisiana continental margin: Effects of major depositional/transport pathways and Hurricane Ivan. Cont. Shelf Res. **28:** 2472–2487, doi:10.1016/j.csr.2008.06.009

Tester, P. A., S. M. Varnam, M. E. Culver, D. L. Eslinger, R. P. Stumpf, R. N. Swift, J. K. Yungel, M. D. Black, and R. W. Litaker. 2003. Airborne detection of ecosystem responses to an extreme event: Phytoplankton displacement and abundance after hurricane induced flooding in the Pamlico–Albemarle Sound system, North Carolina. Estuaries **26:** 1353–1364, doi:10.1007/BF02803637

Wanninkhof, R. 1992. Relationship between wind speed and gas exchange. J. Geophys. Res. **97:** 7373–7382, doi:10.1029/92JC00188

———, W. E. Asher, D. T. Ho, C. Sweeney, and W. R. McGillis. 2009. Advances in quantifying air–sea gas exchange and environmental forcing. Annu. Rev. Mar. Sci. **1:** 213–244, doi:10.1146/annurev.marine.010908.163742

Weiss, R. 1974. Carbon dioxide in water and seawater: The solubility of a non-ideal gas. Mar. Chem. **2:** 203–215, doi:10.1016/0304-4203(74)90015-2

Wetz, M. S., and D. W. Yoskowitz. 2013. An 'extreme' future for estuaries? Effects of extreme climatic events on estuarine water quality and ecology. Mar. Pollut. Bull. **69:** 7–18, doi:10.1016/j.marpolbul.2013.01.020

Whipple, A. C., R. A. Luettich, and H. E. Seim. 2006. Measurements of Reynolds stress in a wind-driven lagoonal estuary. Ocean Dynamics **56:** 169–185, doi:10.1007/s10236-005-0038-x

Woolf, D., I. Leifer, P. Nightingale, T. Rhee, P. Bowyer, G. Caulliez, G. De Leeuw, S. E. Larsen, M. Liddicoat, and J. Baker. 2007. Modelling of bubble-mediated gas transfer: Fundamental principles and a laboratory test. J. Mar. Syst. **66:** 71–91, doi:10.1016/j.jmarsys.2006.02.011

Yoon, B., and P. A. Raymond. 2012. Dissolved organic matter export from a forested watershed during Hurricane Irene. Geophys. Res. Lett. **39:** L18402, doi:10.1029/2012GL052785

Associate editor: Peter Hernes

Received: 24 January 2014
Amended: 28 May 2014
Accepted: 18 June 2014